Detection of luminescence of radicals from TiO$_2$ plate during alpha particle irradiation

Seiichi Yamamoto[*]
Nagoya University Graduate School of Medicine,
Department of Integrated Health Science, Nagoya, Japan

Abstract

Significance: A significant amount of radical related luminescence is observed from the titanium dioxide (TiO$_2$) plate during irradiation of alpha particles although alpha particles do not emit Cerenkov-light.

Aim: TiO$_2$ is a promising material for application to photodynamic therapy in combination with positron radionuclides that emit Cerenkov light. However, it is not clear that radicals are produced by the irradiation of alpha particles, since although Cerenkov light is required to produce radicals, alpha particles do not produce Cerenkov light.

Approach: To clarify this point, the author irradiates alpha particles to a TiO$_2$ plate and measured the produced luminescence of the plate, which indicates the radical production in TiO$_2$.

Results: A significant amount of luminescence was observed from the TiO$_2$ plate during irradiation of alpha particles. The spectrum of luminescence from the TiO$_2$ plate during this irradiation was the same as that emitted by ultraviolet (UV) light irradiated luminescence, which actually showed radical production in a TiO$_2$ plate. This luminescence was not attributed to the UV light from the air scintillation by alpha particles but to the direct irradiation of alpha particles to the TiO$_2$ plate.

Conclusions: A significant amount of luminescence from TiO$_2$ plate was detected during irradiation of alpha particles. The luminescence is thought to be emitted from the radicals produced by the direct alpha particle irradiation to the TiO$_2$ plate.

1 Introduction

Titanium dioxide (TiO$_2$) is an attractive and promising material for its applications to environmental fields with its photocatalysis characteristics via irradiation of ultraviolet (UV) light.[1–10] Furthermore, in biomedical research fields, TiO$_2$ powder offers a promising sensitizer for therapies in combination with UV light[11] and ultrasound irradiation.[12,13] A photodynamic therapy using TiO$_2$ nanoparticles combined with Cerenkov-light irradiation from positrons was also reported.[14,15] In these works of photodynamic therapy, positron emitters and TiO$_2$ nanoparticles are injected into mice with tumors, and the mice injected with both of these showed longer survival times. Here, the mechanism of therapy was explained as follows. UV light in Cerenkov light from positrons produced radicals in the tumor of a mouse where TiO$_2$ nanoparticles had accumulated, and the tumor was killed by the radicals. However, this explanation has faced the criticism that the intensity of Cerenkov light from positrons is too small to produce enough radicals from the TiO$_2$ particles for therapy. The low intensity of Cerenkov light produces a

*Address all correspondence to Seiichi Yamamoto, E-mail: s-yama@met.nagoya-u.ac.jp
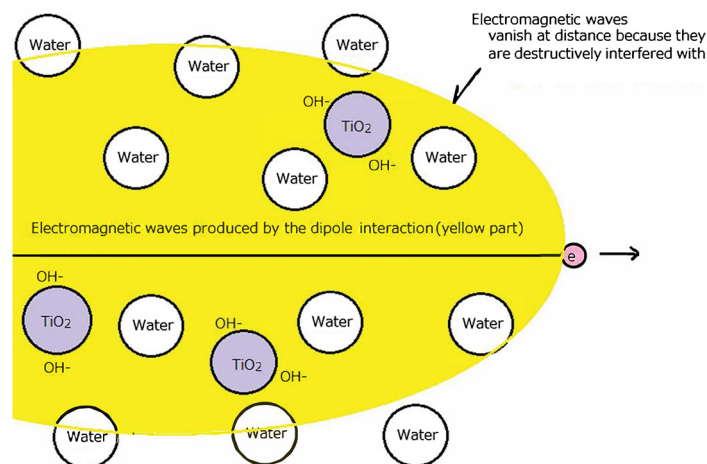
Fig. 1 Conceptual illustration of producing radicals by electromagnetic waves (luminescence of water at lower energy than Cerenkov-light threshold) and TiO$_2$.

small number of radicals from TiO$_2$, thus it is difficult for this viewpoint to explain the effectiveness of positron-based photodynamic therapy.[16] Consequently, another mechanism of producing radicals is needed to explain the effectiveness of these photodynamic therapies using radionuclides.

Recently, the author found luminescence of water at a lower energy than the Cerenkov-light threshold.[17–20] The luminescence had a similar light spectrum to that of Cerenkov light and is thought to be produced by the same mechanism as Cerenkov light: electromagnetic waves produced by the dipole interaction of moving electrons with water molecules at lower energy than the Cerenkov-light threshold.[21] Although the intensity of the luminescence of water is low from a distance, the original electromagnetic wave intensity produced by the dipole interaction of moving electrons with water molecules at the produced points is thought to be much higher than the observed light as schematically shown in Fig. 1. However, the intensity of the electromagnetic waves (light) are reduced at a distant point because the electromagnetic waves are incoherent and emitted almost simultaneously, thus the electromagnetic waves interfere with each other destructively and almost no electromagnetic waves are observed from a distance.[22,23] The luminescence of water found by the author was the small amount of remaining electromagnetic waves that were believed to be invisible from a distance before the author discovered the light.[21–23]

The author realized that the intensity of the produced electromagnetic waves (original light of luminescence lower than Cerenkov light threshold) before vanishing must be very high, much higher than Cerenkov light. This is attributed to Cerenkov light being produced from only a small fraction of the original produced light.[22,23] Because the moving electron produces the electromagnetic waves by interaction with electrons in molecules, if TiO$_2$ particles exist near the electron as shown in Fig. 1, the electromagnetic waves reacting with TiO$_2$ particles produce many radicals before vanishing. To clarify whether the proposed mechanism actually occurred, the author directly irradiated alpha particles on a TiO$_2$ plate and measured the produced radicals in the plate using a high-sensitivity cooled charge-coupled device (CCD) camera.

2 Materials and Methods

2.1 *Principle of Detecting Radicals in TiO$_2$ During Irradiation of Alpha Particles*

It is well established that luminescence at a wavelength between 400 and 600 nm emitted from TiO$_2$ during irradiation of UV light reflects the quantity of produced radicals.[24–28] Therefore, the author irradiated alpha particles on a TiO$_2$ plate and measured the luminescence from the plate using a high-sensitivity cooled CCD camera. The author also measured the spectrum of the produced light from the TiO$_2$ plate to confirm that the light is actually from the radicals produced

in TiO$_2$. The intensity of the light emitted during irradiation of the alpha particles was compared with that during irradiation of UV light from the air scintillation of alpha particles, which had almost the same intensity level as Cerenkov light.

2.2 Experimental Set-Up

Figure 2 shows the measurement set up for produced radical intensity and distributions of the TiO$_2$ plate during irradiation of alpha particles. On the americium-241 (Am-241) alpha source covered by an aluminized Mylar film, a plate pasted with TiO$_2$ powder was set. For measuring the light from the TiO$_2$ plate, the image of the TiO$_2$ plate during irradiation of alpha particles was acquired by an electron-multiplied cooled CCD (EM-CCD) camera from above as shown in Fig. 2(a). When measuring the spectrum of the light from TiO$_2$ or the scintillation of air, one of the long-pass filters was set in front of the lens of the EM-CCD camera, which was used to measure the images as shown in Fig. 2(b).

The author measured the luminescence of the TiO$_2$ plate under various conditions. To measure the images of the TiO$_2$ plate during irradiation of alpha particles, the plate was set directly on the Am-241 alpha source as shown in Fig. 3(a). In this case, there is no space between the Am-241 alpha source and the TiO$_2$ plate and the luminescence of the TiO$_2$ plate during irradiation of alpha particles was measured.
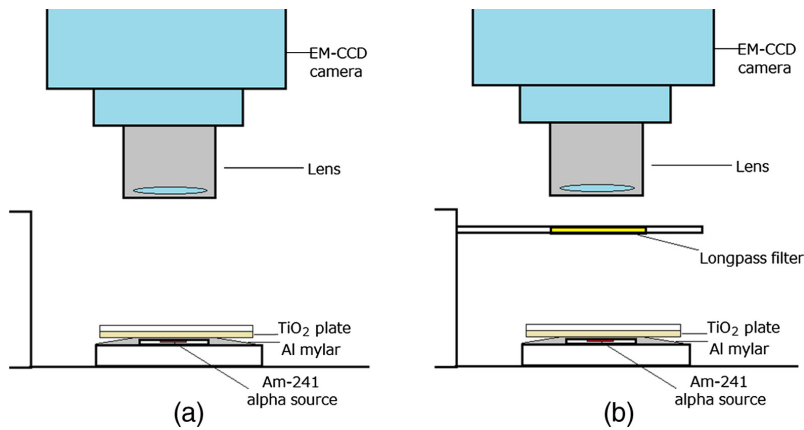

Fig. 2 Set up during measuring produced radical distributions of TiO$_2$ plate during irradiation of alpha particles: (a) without and (b) with optical filter.
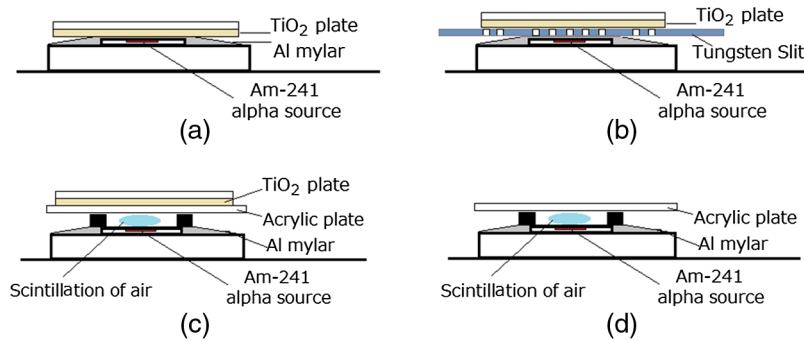

Fig. 3 Set up to measure luminescence images of TiO$_2$ plate under various conditions: (a) standard imaging of luminescence of TiO$_2$ plate during irradiation of alpha particles, (b) imaging of luminescence of TiO$_2$ plate with tungsten plate during irradiation of alpha particles, (c) imaging of luminescence of TiO$_2$ plate during irradiation of scintillation of air, and (d) imaging of scintillation of air.

To check that the position of produced luminescence was the same as the position of the irradiated alpha particles, a thin tungsten plate was set between the Am-241 alpha source and the TiO$_2$ plate as shown in Fig. 3(b). In this case, there was also no space between the Am-241 alpha source and the TiO$_2$ plate, and the luminescence image of the TiO$_2$ plate was measured.

To measure the images of the TiO$_2$ plate by irradiation of UV light from the air scintillation produced by alpha particles, the plate was set on a UV transparent acrylic plate, and the UV light from air scintillation produced by the alpha particles was irradiated to the TiO$_2$ plate as shown in Fig. 3(c). In this case, there was a 2-mm space between the Am-241 alpha source and the UV transparent acrylic plate to produce the air scintillation by alpha particles in this space. The alpha particles were absorbed by the acrylic plate and were not detected by the TiO$_2$ plate. To measure the scintillation of air in the space during irradiation of alpha particles, the TiO$_2$ plate was removed and imaging of the air scintillation was carried out as shown in Fig. 3(d). The imaging of the UV transparent acrylic plate during irradiation of alpha particles was also conducted to check whether the light production by the acrylic plate during irradiation of alpha particles was negligible.

The author also measured the image of a plastic scintillator (NE-102A) during irradiation of alpha particles to quantify the measured intensity of the images assuming the light emission of plastic scintillator for alpha particles is 1000 photons/MeV.

2.3 TiO$_2$ Plate and Alpha Source

TiO$_2$ powder (anatase, average diameter 100 to 150 nm, Nacalai Tesque, Kyoto, Japan) was used for fabricating the TiO$_2$ plate. TiO$_2$ powder was mixed with a binder (polyvinyl alcohol) at a weight ratio of 1:1 and made a uniformly mixed TiO$_2$ solution. On an acrylic plate (25 mm $\times$ 25 mm $\times$ 1.5 mm thick), this TiO$_2$ solution was pasted with a thickness of $\sim$60 μm [Fig. 4(a)]. This was thick enough to absorb all the energy of the alpha particles in TiO$_2$. The imaging of the binder during irradiation of alpha particles was also conducted to check whether the light production of the binder during irradiation of alpha particles was negligible.

The alpha source was Am-241 (5.5 MeV) with an activity of 2-MBq, and the source's active area was 10 mm $\times$ 10 mm. To avoid scintillation of the dust on the source, the active area was covered with an aluminized Mylar film to absorb the light on the source surface [Fig. 4(b)].

The refractive index of TiO$_2$ is 2.52, so Cherenkov light threshold energy is low (46 keV for 2.52). The Cherenkov light threshold is lower than 59 keV, which is the energy of the gamma photons from Am-241 and it is possible to emit Cherenkov light by 59-keV gamma photons. The author checked the intensity of the TiO$_2$ plate during irradiation of 59-keV gamma photons from Am-241 by inserting a black paper between the Am-241 source and TiO$_2$ plate to absorb alpha particles and compared the intensities with that of alpha particles.

2.4 Imaging System

The imaging system used to measure the luminescence of a TiO$_2$ plate is shown in Fig. 5(a). The system used for the imaging was a cooled EM-CCD camera (ImagEM, Hamamatsu Photonics,
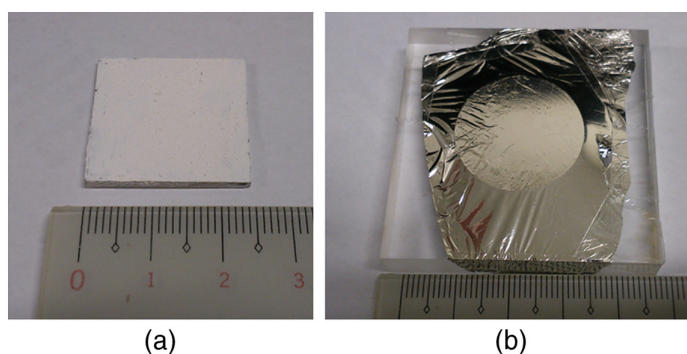

(a)　　　　　　　　　(b)

Fig. 4 Photo of fabricated (a) TiO$_2$ plate and (b) alpha source used for imaging experiments.
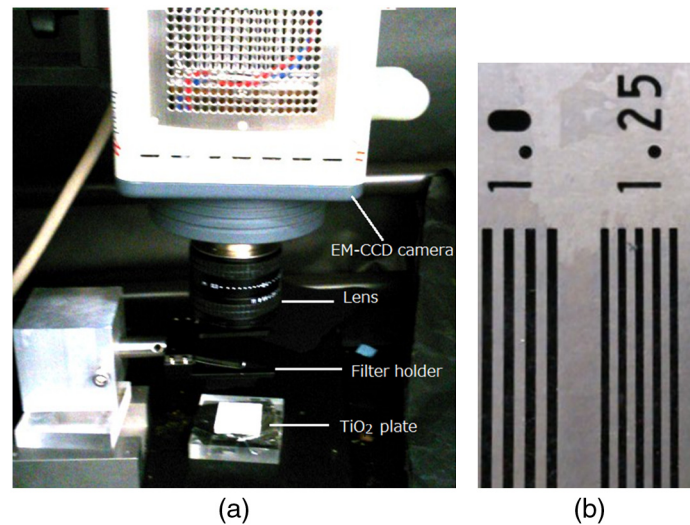
(a)　　　　　　　　　　(b)

Fig. 5 (a) Photo of imaging system to measure luminescence of TiO$_2$ plate and (b) photo of tungsten slits.

Japan) operating at $-65°C$ with a C-mount F-0.95 lens set ~8 cm from the source surface. An extension ring was used between the lens and the camera. Acquisition was conducted with 2×2 binning at a matrix size of 256×256. Each image was acquired for 10 s. The system was set in a dark box to shut out environmental light. The tungsten slits used for the imaging are shown in Fig. 5(b). The slit widths were 0.5 mm (1.0 line pair/mm) and 0.4 mm (1.25 line pair/mm), and the thickness was ~0.1 mm.

The optical filters used were long-pass types longer than 350 nm (Asahi Spectra, LU0350), 450 nm (Asahi Spectra, LV0450), 550 nm (Asahi Spectra, LV0550), 650 nm (Asahi Spectra, LV0650), and 750 nm (Asahi Spectra, LI0750). The subtracted images were calculated from these images to produce bandpass images of 350 to 450 nm, 450 to 550 nm, 550 to 650 nm, and 650 to 750 nm. The intensities of these images were corrected for sensitivity distribution of the CCD camera and transmission of the lens and the light spectra were derived.

2.5 *Image Processing*

The acquired images were processed using public domain software (ImageJ). Noise spots due to the direct absorption of gamma photons by the CCD image sensor were eliminated using high-intensity and small-pixel information. A blank image was measured without light at the same acquisition time and then subtracted from each luminescence image for the correction of the offset value of the luminescence image. After setting a region of interest (ROI) on the luminescence part of each image, the average pixel value was calculated. The size of the ROI was ~7 mm $\times$ 7 mm.

3 Results

One of the luminescence images of the TiO$_2$ plate during irradiation of alpha particles is shown in Fig. 6(a). The position where the alpha source directly contacts the TiO$_2$ plate was imaged. The nonuniform distribution of the luminescence was due to the TiO$_2$ plate's nonuniformity. The luminescence intensities with and without an alpha source as a function of elapsed time after closing the dark box is shown in Fig. 6(b). In the image of the first frame, the background intensity was observed without a source at a level of 3% of that with a source. However, the background intensity of the TiO$_2$ plate decreased to ~1% of that with the alpha source.

A luminescence image of the TiO$_2$ plate with a tungsten slit during irradiation of alpha particles is shown in Fig. 7(a). The profile of the image in the horizontal direction is shown in Fig. 7(b). The slit shape was clearly observed, and the 0.5-mm slits (left part of profile) were
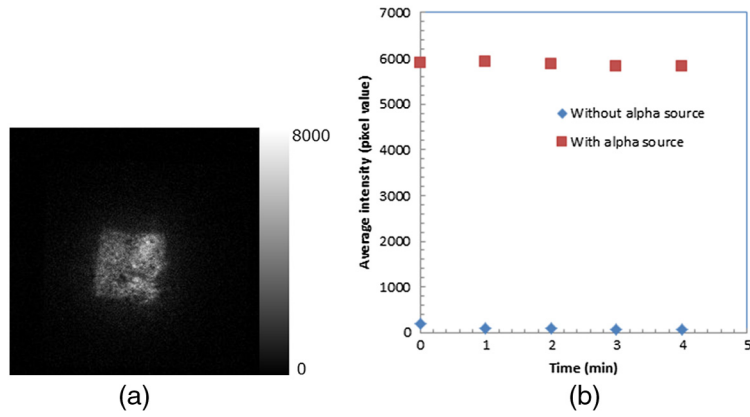
Fig. 6 (a) Luminescence image of TiO$_2$ plate during irradiation of alpha particles and (b) luminescence intensities with and without alpha source as a function of elapsed time after closing the dark box.
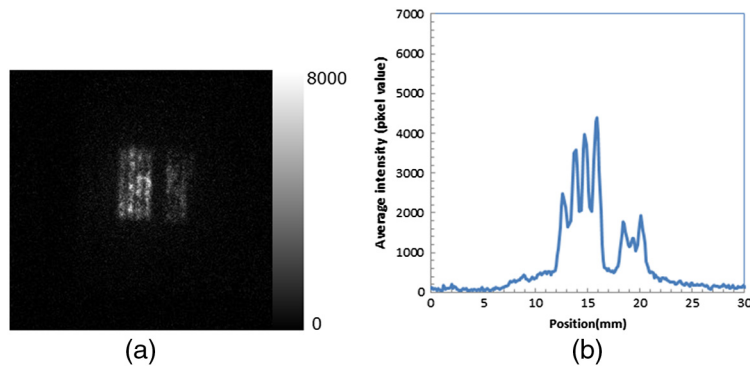

Fig. 7 (a) Luminescence image of TiO$_2$ plate with tungsten slit during irradiation of alpha particles and (b) profile of image in the horizontal direction.

clearly resolved. The luminescence of the binder (polyvinyl alcohol) during irradiation of alpha particles was negligible (~4% of the luminescence of TiO$_2$). The intensity of the TiO$_2$ plate during irradiation of the gamma photons (59 keV) from Am-241 was 1.5% of that during irradiation of alpha particles and it was also negligible.

Figure 8(a) shows the light spectra of TiO$_2$ luminescence during the irradiation of alpha particles. The spectrum shows a peak around 500 nm, which was the same as the UV-irradiated spectrum of TiO$_2$,[24–28] indicating that the produced luminescence was the radicals produced in the TiO$_2$ plate.

Figure 8(b) shows the light spectra of scintillation of air during irradiation of alpha particles to air. The spectrum shows a peak around 400 nm, which was the same as the light spectrum of air scintillation during alpha particle irradiations.[29] Since the scintillation of air contained UV light shorter than 360 nm,[29] it could be used for UV light to irradiate the TiO$_2$ plate.

Figure 9(a) shows the scintillation of air during irradiation of alpha particles. We could observe the blurred image of the scintillation of air. Figure 9(b) shows the luminescence of the TiO$_2$ plate during irradiation of scintillation of air. The luminescence of the TiO$_2$ plate during irradiation of scintillation of air was nearly invisible as shown in Fig. 9(b).

Table 1 summarizes the average intensities of luminescence of the TiO$_2$ plate during irradiation of alpha particles and scintillation of air. The intensity of the luminescence of the TiO$_2$ plate during irradiation of scintillation of air was only 1.6% of that during irradiation of alpha particles. The luminescence of the acyclic plate during irradiation of alpha particles was negligible (~4% of the luminescence of TiO$_2$).
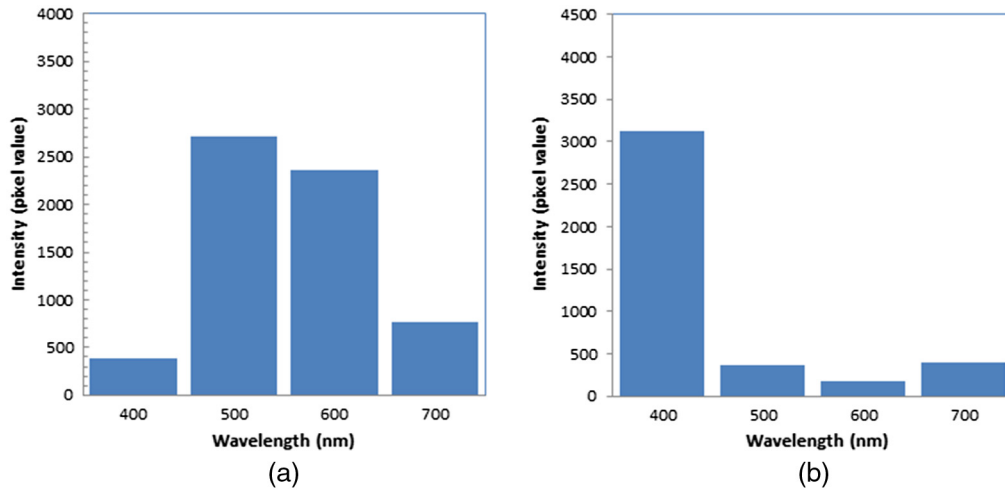
Fig. 8 Light spectra of TiO₂ luminescence during irradiation of (a) alpha particles and (b) scintillation of air.
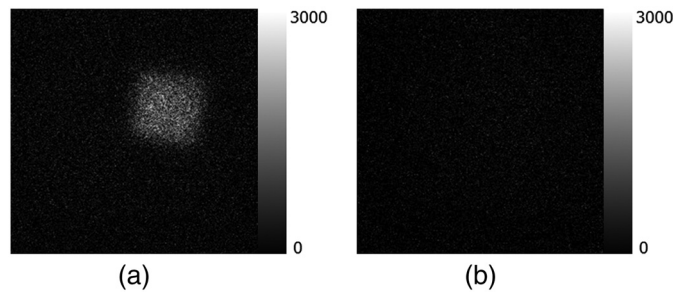

Fig. 9 (a) Scintillation of air during irradiation of alpha particles and (b) luminescence of TiO₂ plate during irradiation of scintillation of air.

Table 1 Average intensities of luminescence of TiO₂ plate during irradiation of alpha particles and scintillation of air.

	Scintillation of air	TiO₂ plate during irradiation of alpha particles	TiO₂ plate during irradiation of scintillation of air
Average intensity	1050	5822	96
Ratio (alpha irradiation: 100%)	18	100	1.6
Photons/MeV	11	59	0.9
Photons/5.5 MeV alpha particle	61	326	5

4 Discussion

We measured the luminescence of a TiO₂ plate during irradiation of alpha particles. The spectrum shown in Fig. 8(a) indicated that the luminescence of the TiO₂ plate was attributed to the produced radicals in the TiO₂ plate. The extremely small luminescence of the TiO₂ plate during irradiation of the scintillation of air supports the notion that the luminescence of the TiO₂ plate was not produced by the scintillation of air but by the direct irradiation of alpha particles to TiO₂. One possible explanation is that the electromagnetic waves were produced by the dipole

interaction of moving electrons with TiO_2 or binder molecules; that was the origin of the luminescence of water and Cerenkov light.[21–23] The electromagnetic waves are thought to vanish due to destructive interference with each other at a very close distance to the electron trajectory, but a certain distance is still needed for the waves to interfere with each other before vanishing. If the waves need one wavelength of the light to interfere with each other, the electromagnetic waves remain within $\sim$500 nm from the electron trajectory. Within that area, TiO_2 particles produce radicals by the irradiation of the UV light in the electromagnetic waves.

The intensity of the scintillation of air during irradiation of alpha particles is $\sim$15 photons/MeV (Ref. 19) and the measured scintillation of air was 11 photons/MeV listed in Table 1, which is comparable intensity to that of Cerenkov light ($\sim$20 photons) from positrons.[30,31] When a similar intensity to Cerenkov light was irradiated to the TiO_2 plate using the scintillation of air, almost no luminescence from radicals was observed in the TiO_2 plate. This suggests that the radical production by positrons as previously reported[14] was not from the Cerenkov light but might be attributed to the electromagnetic waves produced by the dipole interaction of moving positrons interacting with TiO_2.

The luminescence intensities after closing the dark box were stable with and without an alpha source as shown in Fig. 6(b), indicating that the luminescence of the TiO_2 plate was not from the phosphorescence by the irradiation of room light before measurement. There was very small phosphorescence (3% of the luminescence by the irradiation of alpha particles) observed in the TiO_2 plate, but it still decreased within 1 min. Furthermore, it became obvious that the radical production in the TiO_2 plate was stable during irradiation of alpha particles because the intensity of the luminescence was the same as shown in Fig. 6(b).

The luminescence image of the TiO_2 plate with a tungsten slit during irradiation of alpha particles (Fig. 7) suggests that the radicals in the TiO_2 plate were generally produced only in the areas where alpha particles were directly irradiated. This is good for photodynamic therapy because radicals are produced only in the areas where alpha particles are irradiated, not in other areas.

From the results of these measurements, radicals can be produced by other types of radiations such as those of beta particles, gamma photons, and x-rays. In the proposed mechanism, there is not a threshold energy of radiations to produce radicals. The radical production by irradiation of x-rays to TiO_2 was previously reported.[32] The author thinks that the radical production by irradiation of x-rays to TiO_2 was attributed to the same mechanism as that of alpha particle irradiation occurring in TiO_2.

5 Conclusion

A significant amount of luminescence from a TiO_2 plate was observed during irradiation of alpha particles. The spectrum of the luminescence confirmed that this was from the radicals produced in TiO_2. The luminescence was produced by the direct alpha particle irradiation to the TiO_2 plate. With these results, alpha particles emitting radionuclides may have a potential for use in photodynamic therapy.

Disclosures

The author has no conflicts of interest in this manuscript.

Acknowledgments

References

1. A. Fujishima and K. Honda, "Electrochemical photolysis of water at a semiconductor electrode," *Nature* **238**, 37 (1972).

2. M. Fujihira, Y. Satoh, and T. Osa, "Heterogeneous photocatalytic oxidation of aromatic compounds on TiO₂," *Nature* **293**, 206 (1981).
3. K. Hashimoto, H. Irie, and A. Fujishima, "TiO₂ photocatalysis: a historical overview and future prospects," *Jpn. J. Appl. Phys.* **44**(12), 8269–8285 (2005).
4. K. Sunada et al., "Bactericidal and detoxification effects of TiO₂ thin film photocatalysts," *Environ. Sci. Technol.* **32**(5), 726–728 (1998).
5. P. Sawunyama et al., "Photodecomposition of a Langmuir–Blodgett film of stearic acid on TiO₂ film observed by in situ atomic force microscopy and FT-IR," *J. Phys. Chem. B* **101**, 11000–11003 (1997).
6. Y. Ohko et al., "Photoelectrochemical anticorrosion and self-cleaning effects of a TiO₂ coating for type 304 stainless steel," *J. Electrochem. Soc.* **148**, B24 (2001).
7. A. Fujishima, K. Hashimoto, and T. Watanabe, *TiO₂ Photocatalysis: Fundamentals and Applications*, BKC, Tokyo (1999).
8. T. Tatsuma, W. Kudo, and A. Fujishima, "Patterning of solid surfaces by photocatalytic lithography based on the remote oxidation effect of TiO₂," *Langmuir* **18**, 9632 (2002).
9. A. Nakajima et al., "Transparent superhydrophobic thin films with self-cleaning properties," *Langmuir* **16**, 7044 (2000).
10. B. O'Regan and M. Grätzel, "A low-cost, high-efficiency solar cell based on dye-sensitized colloidal TiO₂ films," *Nature* **353**, 737 (1991).
11. F. U. Rehman et al., "Biomedical applications of nano-Titania in theranostics and photo-dynamic therapy," *Biomater. Sci.* **4**, 40–54 (2016).
12. Y. Harada et al., "Ultrasound activation of TiO₂ in melanoma tumors," *J. Control Release Jan* **149**(2), 190–195 (2011).
13. D. G. You et al., "ROS-generating TiO₂ nanoparticles for non-invasive sonodynamic therapy of cancer," *Sci. Rep.* **6**, 23200 (2016).
14. N. Kotagiri et al., "Breaking the depth dependency of phototherapy with Cerenkov radiation and low-radiance-responsive nanophotosensitizers," *Nat. Nanotechnol.* **10**(4), 370–379 (2015).
15. J. Grimm, "Therapy from within," *Nat. Nanotechnol.* **10**, 299–300 (2015).
16. G. Pratx and D. S. Kapp, "Is Cerenkov luminescence bright enough for photodynamic therapy?" *Nat. Nanotechnol.* **13**, 354 (2018).
17. S. Yamamoto et al., "Luminescence imaging of water during proton-beam irradiation for range estimation," *Med. Phys.* **42**(11), 6498–6506 (2015).
18. S. Yamamoto et al., "Luminescence imaging of water during carbon-ion irradiation for range estimation," *Med. Phys.* **43**, 2455–2463 (2016).
19. S. Yamamoto et al., "Luminescence imaging of water during alpha particle irradiation," *Nucl. Instrum. Methods Phys. Res. Sec. A* **819**(21), 6–13 (2016).
20. S. Yamamoto et al., "Luminescence imaging of water during irradiation of x-ray photons lower energy than Cerenkov light threshold," *Nucl. Instrum. Methods Phys. Res. Sec. A* **832**, 264–270 (2016).
21. S. Yamamoto et al., "Source of luminescence of water lower energy than the Cerenkov-light threshold during irradiation of carbon-ion," *J. Phys. Commun.* **2**, 065010 (2018).
22. J. V. Jelley, *Cherenkov Radiation and its Applications*, Pergamon, Oxford (1958).
23. J. V. Jelley, "Cerenkov radiation and its applications," *Br. J. Appl. Phys.* **6**, 227 (1955).
24. M. Anpo, T. Shima, and Y. Kubokaw, "ESR and photoluminescence evidence for the photocatalytic formation of hydroxyl radicals on small TiO₂ particles," *Chem. Lett.* **14**(12), 1799–1802 (1985).
25. A. Masakazu and T. Masanori, "In situ photoluminescence of titania as a probe of photo-catalytic reactions," *J. Phys. Chem.* **93**, 7300–7302 (1989).
26. Y. Nakaoka and Y. Nosaka, "ESR investigation into the effects of heat treatment and crystal structure on radicals produced over irradiated TiO₂ powder," *J. Photochem. Photobiol. A* **110**(3), 299–305 (1997).
27. D. K. Pallotti et al., "Photoluminescence mechanisms in anatase and rutile TiO₂," *J. Phys. Chem. C* **121**, 9011–9021 (2017).
28. A. Stevanovic and J. T. Yates, "Electron hopping through TiO₂ powder: a study by photo-luminescence spectroscopy," *J. Phys. Chem. C* **117**(46), 24189–24195 (2013).

29. J. Sand et al., "Imaging of alpha emitters in a field environment," *Nucl. Instrum. Methods A* **782**(11), 13–19 (2015).
30. G. Knoll, *Radiation Detection and Measurement*, Chapter 19, 3rd ed. (2000).
31. E. Ciarrocchi and N. Belcari, "Cerenkov luminescence imaging: physics principles and potential applications in biomedical sciences," *EJNMMI Phys.* **4**, 14 (2017).
32. K. Tamura et al., "X-ray induced photoelectrochemistry on TiO₂," *Electrochim. Acta* **52**(24), 6938–6942 (2007).

A biography of the author is not available.